Draft genome of *Trichoderma gamsii* strain T035 a promising beneficial fungus in agriculture

Justine Colou[1], Alwena Robin[1], Franck Bastide[1], Thomas Guillemette*[1]

[1] Institut Agro, University Angers, INRAE, IRHS, SFR 4207 QuaSaV, F-49000 – Angers, France

*Corresponding author
Correspondence: thomas.guillemette@univ-angers.fr

ABSTRACT

Trichoderma gamsii is a filamentous fungus widely recognized for its beneficial roles in agriculture, particularly for its ability to suppress plant pathogens and enhance crop health. However, genomic resources for this species remain scarce, limiting functional and applied studies. Here, we report the high-quality draft genome of *T. gamsii* strain T035, a promising biocontrol strain with strong antibiosis and parasitic activities against diverse pathogens. The assembly consisted of 18 scaffolds, with an N50 value of 7.2 Mb and a total assembly length of 38.8 Mb. This draft genome represents the most complete *T. gamsii* assembly to date and will provide a valuable resource to facilitate the exploration of molecular mechanisms underlying biocontrol and support the development of sustainable plant protection strategies.

Keywords: *Trichoderma*, biocontrol, genome, annotation, Helixer, transposable elements, secondary metabolites

Introduction

The genus *Trichoderma* belongs to the phylum Ascomycota in the family Hypocreaceae. *T. gamsii* is a ubiquitous fungus found in diverse environments, where it can exhibit psychrotolerance and broad pH tolerance (Migheli et al., 2009; Rinu et al., 2014). This species is particularly interesting due to its ability to suppress pathogens through enzymatic activity and the release of volatile organic compounds (Anees et al., 2010; Chen et al., 2016; Galletti et al., 2020; Bedine Boat et al., 2020; Valan Arasu et al., 2023; Marik et al., 2025). Additionally, it promotes plant health by inducing systemic resistance and stimulating plant growth (Anees et al., 2010; Rinu et al., 2014; Chen et al., 2016; Galletti et al., 2020; Valan Arasu et al., 2023). Those characteristics highlight the potential of *T. gamsii* for biotechnological applications, making the availability of comprehensive genomic data of utmost importance to further investigate its biocontrol abilities. To date, the best public genomic sequence available for this species belongs to the strain T6085, which is known for its ability to control *Fusarium* head blight on wheat (Baroncelli et al., 2016).

In this study, we performed *de novo* sequencing of *T. gamsii* T035 genome. This strain exhibits strong antagonistic activity against multiple plant pathogens, making it a promising model to explore *T. gamsii* biocontrol potential. Here, we present a high-quality genome assembly and functional annotation, representing the most contiguous *T. gamsii* genome available to date, and a resource to support future comparative and applied studies.

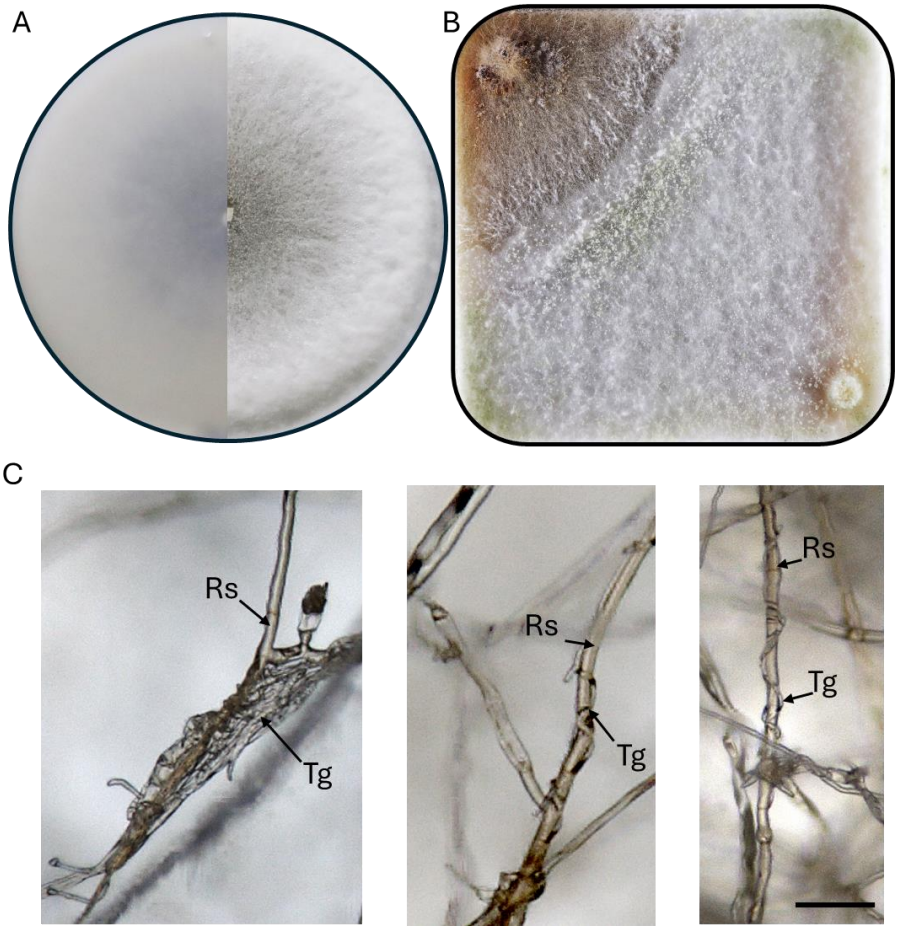

Figure 1 - Colony morphology of *Trichoderma gamsii* T035 on PDA after 7 days of growth (A). Confrontation assay between T035 and PAT-009 (*Rhizoctonia solani*) (B). Hyphal coiling of *Trichoderma* T035 (Tg) around PAT-009 (Rs) (scale bar = 50 µm) (C).

Material and methods

Sample information

Trichoderma gamsii strain T035 was isolated in 2019 from carrot-cultivated soil in Brain-sur-l'Authion, France (GPS coordinates: latitude 47.473936; longitude −0.390684) (Fig.1). Sampling and isolation were performed following the method described by Chateau et al. (2024). Briefly, 5 g of rhizosphere soil were suspended in 50 mL of sterile water. Serial dilution–extinction was carried out on Potato Dextrose Agar (PDA; Grosseron, 39 g L^{-1}) supplemented with streptomycin (500 mg L^{-1}). Cultures were incubated in darkness at 20 °C for seven days. Strain T035 was subsequently transferred to Malt Agar medium (MA; Grosseron, 20 g L^{-1} bacteriological malt extract, 15 g L^{-1} bacteriological agar type A) and maintained under the same growth conditions. For long-term preservation, mycelial explants were stored at −80 °C in 30% glycerol solution as a cryoprotectant.

Trichoderma atroviride strain I1237 was obtained from the commercial product TRI-SOIL® (Agrauxine, Beaucouzé, France).

Pathogenic strains were sourced either from our laboratory fungal collection (IRHS, FungiSem Team, Beaucouzé, France) or from the CIRM-CFBP collection (Beaucouzé, France). A summary of pathogen strains used in this study is provided in Supplementary Table SI.

In vitro control of filamentous pathogens

The two *Trichoderma* isolates were evaluated for their mycoparasitic activity against twelve pathogenic fungal isolates using the dual culture assay (Bunbury-Blanchette & Walker, 2019). Square Petri dishes (120 × 120 mm) containing PDA medium were inoculated with two 5 mm mycelial plugs: one obtained from a pathogen colony and the other from a *Trichoderma* colony previously grown on PDA under the conditions described above. The plugs were placed at opposite corners of the plate, with the pathogen inoculated two days before the antagonist. Control plates consisted of single-pathogen plugs grown on PDA alone. Each condition was replicated three times, and the entire experiment was repeated independently three times.

Plates were incubated in darkness at 20 °C for 20 days. Mycoparasitic ability was visually assessed using a scale adapted from Pascouau et al. (2023): 0 = <5% of pathogen colony overgrown by *Trichoderma*; 1 = 5–25% overgrown; 2 = 25–50% overgrown; 3 = 50–75% overgrown; 4 = >75% overgrown (Figure S1).

Statistical analyses were performed in RStudio v2023.12.1. Data were analyzed using a non-parametric analysis of variance (Wilcoxon signed-rank test), and *p*-values were adjusted for multiple testing using the false discovery rate (FDR) method.

In vitro control of bacterial pathogens

Two *Trichoderma* isolates were assessed for their antibiosis capacity against two bacterial isolates following the protocols of Dennis & Webster (1971) and Lee et al. (2012), with modifications. For each *Trichoderma* isolate, 250 mL Erlenmeyer flasks containing 50 mL of Potato Dextrose Broth (PDB, Grosseron, 24 g L^{-1}, pH 5.2) were inoculated with five mycelial plugs (5 mm diameter) taken from 7-day-old PDA cultures. Cultures were incubated at 20 °C on a rotary shaker (100 rpm) for 7 days and subsequently filtered through sterile 0.2 µm syringe filters (ClearLine®, Dutscher) to obtain culture filtrates.

The effect of the filtrates on bacterial growth was evaluated using a spectrophotometric microplate assay (96-well plates, SPECTROstar, BMG Labtech). Autoclaved Lysogeny Broth (LB, Grosseron, 24 g L^{-1}) was inoculated with 1% (v/v) of a bacterial suspension adjusted to OD = 0.05, supplemented with 10% (v/v) of *Trichoderma* culture filtrates, in a final volume of 300 µL per well. Filtrates obtained from non-inoculated PDA disks were incubated under the same conditions and served as controls. Plates were incubated at 25 °C for 33 h with intermittent shaking (5 min at 200 rpm every 10 min), and absorbance at 600 nm was recorded every 10 min.

Each condition was tested in triplicate, and three independent experiments were conducted. The area under the growth curve was calculated as described by Joubert et al. (2010) and Warringer & Blomberg (2003). Data were analyzed using analysis of variance (ANOVA) followed by Tukey's multiple comparisons test (α = 0.05).

Trichoderma genome comparison

A global comparison of *Trichoderma* genomes was performed using MashTree v1.2 (Katz et al., 2019). Genome assemblies of *T. gamsii* and representative assemblies from other *Trichoderma* species were retrieved from NCBI RefSeq (accessions listed in Supplementary Table S2).

Pairwise genomic distances were computed with Mash (genome size parameter set to 40 Mb, sketch size = 20,000). The distance matrix was used to infer a neighbor-joining tree with MashTree. The obtained tree was exported in Newick format, and later visualized and annotated using MEGA12 (Kumar et al., 2024) (Fig.2).

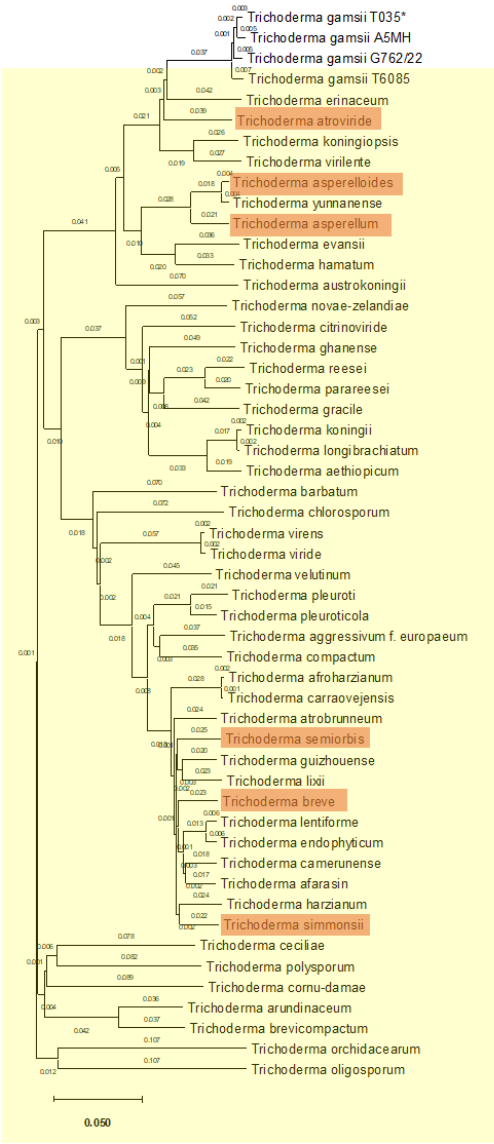

Figure 2: Mashtree phylogeny of *Trichoderma* genomes. The analysis included all reference *Trichoderma* genomes available in NCBI (yellow) as well as all known *T. gamsii* genomes. The genome obtained in this study is indicated with an asterisk. Complete genomes are highlighted in orange.

120

121 **DNA extraction**

122 High-molecular-weight genomic DNA was extracted from a 7-day-old culture of *T. gamsii* T035
123 grown on a pectocellulosic membrane placed on PDA medium. Tissues were frozen with liquid
124 nitrogen and bead-milled. DNA extraction followed an adapted Möller protocol: RNase treatment
125 was performed immediately after proteinase K digestion, and DNA was resuspended in 10 mM
126 Tris (pH 8) instead of TE buffer, as EDTA can interfere with Nanopore sequencing (Möller et al.,
127 1992). The A260/280 and A260/230 ratios were 1.85 and 2.3, respectively. DNA concentration
128 was measured using the quBit to 27 ng/µL, and its integrity was confirmed by electrophoresis gel,
129 where the majority of the gDNA was above 10 kilobases (kb) in length.

130 **Oxford Nanopore Technologies (ONT) sequencing**

131 The sequencing library was prepared using the Native Barcoding Kit 96 V14 (SQK-NBD114.96)
132 with 1.5 µg of high-molecular-weight genomic DNA as described in the kit protocol. We performed
133 *de novo* sequencing of *T. gamsii* T035 genome using Oxford Nanopore Technologies' MinION
134 device (Lu et al., 2016).

135 **Genome assembly**

136 Reads were basecalled using the super accuracy (SUP) mode. The long-read assemblies were
137 performed using both Canu v2.2 (Koren et al., 2017) and Flye v2.9.6 (Kolmogorov et al., 2019).
138 The less fragmented assembly was obtained using Flye, with reads filtered before assembly where
139 reads shorter than 1,000 bp or with a quality score below Q10 were removed (De Coster et al.,
140 2018). The assembly underwent three additional polishing steps using Racon (Vaser et al., 2017).
141 The obtained contigs were further assembled in scaffolds using RagTag (Alonge et al., 2022)
142 thanks to the reference genome of *Trichoderma atroviride* (GCF_020647795.1), the
143 phylogenetically closest completed genome to *T. gamsii* (Fig. 2). Assembly quality was later
144 assessed with BUSCO (fungi database) and compared to the reference *T. gamsii* genome
145 (RefSeq: GCF_001481775.2) using QUAST (Mikheenko et al., 2023; Tegenfeldt et al., 2025) (Fig.
146 3 and Table I).

147 Table I: Comparison of global genome metrics of *Trichoderma gamsii* genomes. The
148 asterisk indicates the actual reference genome of *T. gamsii* in NCBI.

ASSEMBLY STATISTICS	*TRICHODERMA GAMSII* STRAIN T6085*	*TRICHODERMA GAMSII* STRAIN A5MH	*TRICHODERMA GAMSII* STRAIN G762/22	TRICHODERMA GAMSII STRAIN T035 (THIS STUDY)
SUBMITTED GENBANK ASSEMBLY	GCA_001481775.2	GCA_002894205.1	GCA_049996675.1	
GENOME SIZE	37.9 Mb	38.5 Mb	38 Mb	38.8 Mb
TOTAL UNGAPPED LENGTH	37.9 Mb	38.5 Mb	38 Mb	38.8 Mb
NUMBER OF SCAFFOLDS	172	292	499	18
SCAFFOLD N50	697.4 kb	594.5 kb	285.3 kb	7.2 Mb
SCAFFOLD L50	18	20	44	3
NUMBER OF CONTIGS	216	517	499	30
CONTIG N50	534 kb	299.2 kb	285.3 kb	3.096 Mb
CONTIG L50	23	42	44	5
GC PERCENT	49	48.5	48.5	48.4
GENOME COVERAGE	50x	90x	35x	25.4x
ASSEMBLY LEVEL	Scaffold	Scaffold	Contig	Scaffold

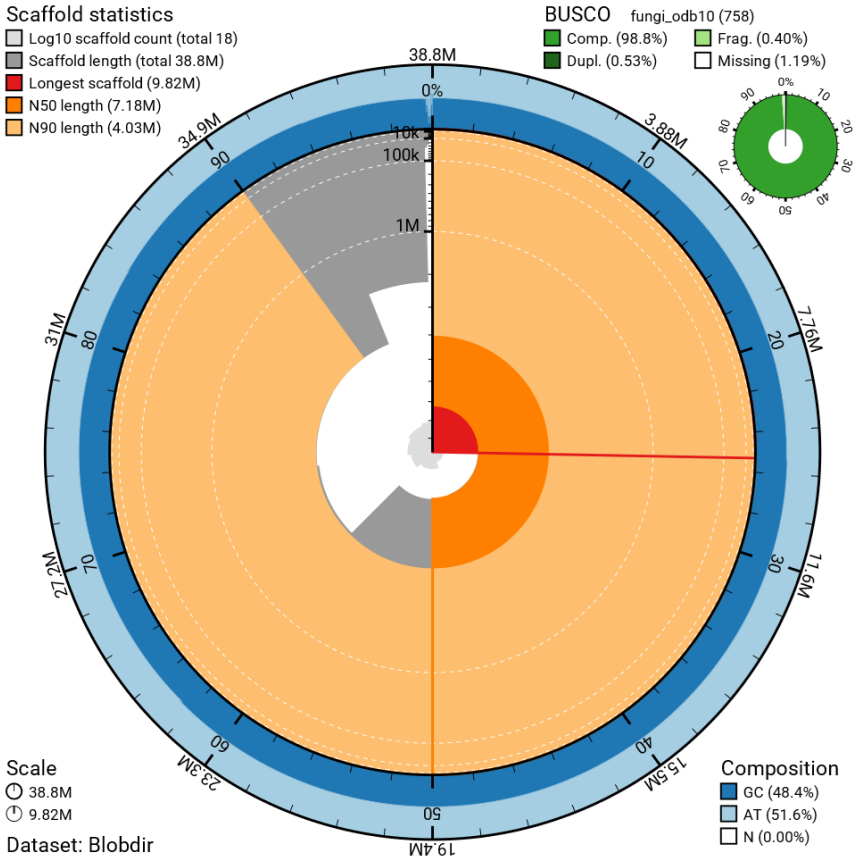

Figure 3: Snailplot generated with BlobToolKit showing assembly statistics for the *Trichoderma gamsii* T035 genome. The assembly has a total length of 38,792,561 bp with a maximum scaffold length of 9,818,134 bp (in red). N50 and N90 sequence lengths are 7,178,191 bp and 4,032,368 bp, indicated by orange and pale-orange arcs, respectively. The grey spiral represents scaffold lengths in descending order on a log scale. BUSCO analysis against the fungi_odb10 dataset indicates 98.8% completeness (top right). The outer ring shows base composition (GC: 48.4%, AT: 51.6%, N: 0.0%). It's important to note that BlobToolKit reports 0.0% N, as the gaps introduced by RagTag during the scaffolding are synthetic and not associated with a raw sequence.

Annotation

Structural annotation was performed using the deep-learning tool Helixer (Holst et al., 2023). This annotation was later confirmed using STAR (Dobin et al., 2013) and public transcriptomic data (Supplementary Table S3). The location of transposable elements in the assembled genome was assessed using EDTA (Su et al., 2021) (Supplementary Table S4).

Functional annotation was carried out with EggNOG-mapper (Cantalapiedra et al., 2021) (Supplementary Table S5), signal peptides were predicted using DeepSig (Savojardo et al., 2018) (Supplementary Table S6), secondary metabolite clusters were identified using antiSMASH 8.0 (Blin et al., 2025) (Supplementary Table S7), and carbohydrate-active enzymes were identified with high confidence (confirmed by HMMER, DIAMOND, and dbCAN_sub) using dbCAN3 (Zheng et al., 2023) (Supplementary Tables S8 and S9). All annotation results are synthesized in the Supplementary Table S10.

Results

Biocontrol assays

The biocontrol potential of *T. gamsii* strain T035 was assessed through its parasitism and antibiosis capacities. Strain T035 displayed greater parasitic activity than the commercial strain I1237 against eight of the twelve tested filamentous plant pathogens (Fig. 4A). Notably, while I1237 exhibited antibiosis activity against both *Acidovorax valerianellae* and *Xanthomonas campestris*, strain T035 was more than twice as effective (Fig. 4B).

An intriguing pattern emerged in the parasitism assays with *Globisporangium* species: strain T035 was particularly effective against isolate PAT-018, but showed markedly reduced activity against the two other *Globisporangium* strains tested (Fig. 4A).

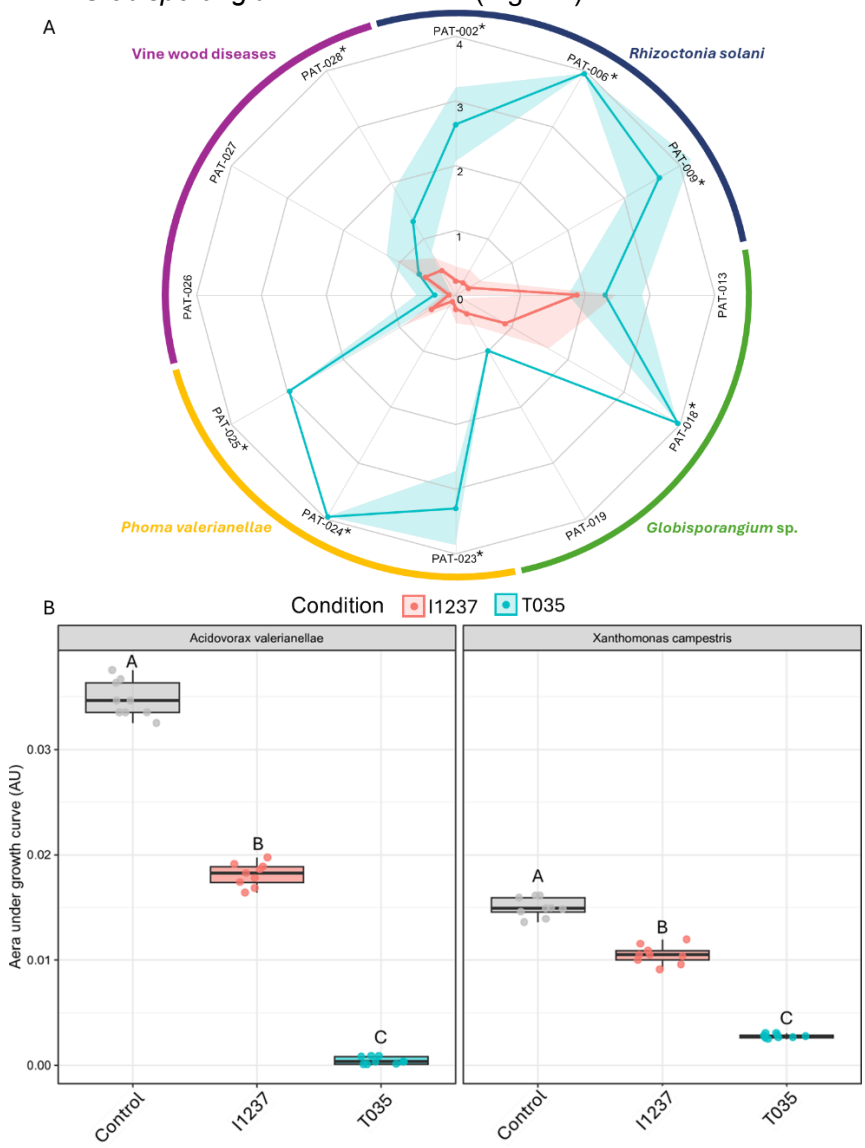

Figure 4: Evaluation of biocontrol capacities of *T. gamsii* strain T035 compared with a commercial *Trichoderma* strain (I1237). (A) Radar plot showing the parasitic capacity of both strains against twelve isolates from four different filamentous plant pathogens. Scores range from 0 (no colonization) to 4 (complete colonization). Asterisks indicate significant differences between strains (Wilcoxon signed-rank test; p-value 0.05). (B) Boxplot showing the growth of two phytopathogenic bacteria under control conditions (grey) or after exposure to culture filtrates of strain I1237 (pink) and *T. gamsii* T035 (blue). Different letters indicate significant differences according to Tukey's multiple comparisons test (α = 0.05).

Genome sequencing and assembly results

ONT sequencing of *T. gamsii* strain T035 generated 196,604 reads with a N50 read length of 6,669 bp, yielding approximately 965 Mb of sequence data, which corresponds to around 25X genome coverage (Fig. 5). The median read quality and length were respectively 21.8 and 3,217 bp.

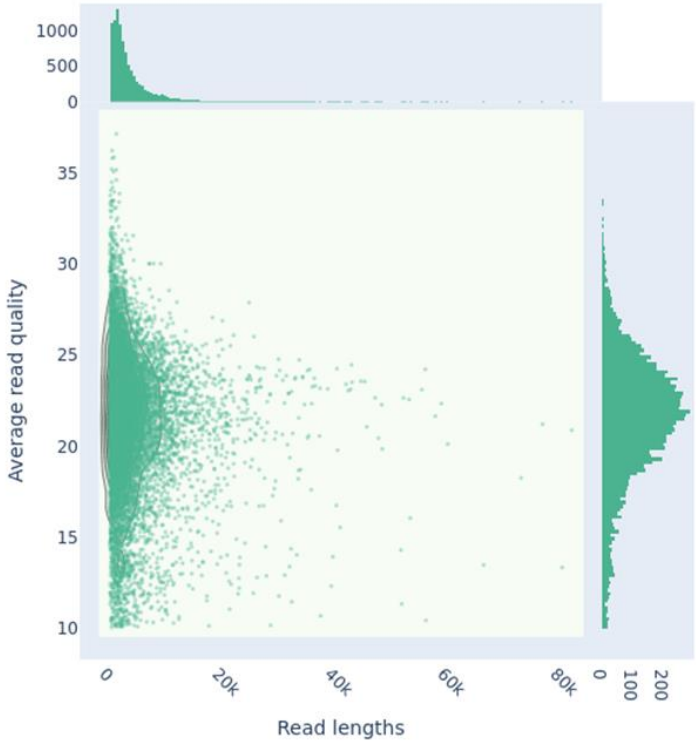

Figure 5: Scatterplot of Nanopore reads for *T. gamsii* strain T035, showing read length versus quality score, generated with NanoPlot (kde plot). A total of 196,604 reads were analyzed, representing approximately 965 Mbp of sequence data. The read length N50 is 6,669 bp, with a median read length of 3,217 bp, while the median read quality is 21.8.

The obtained genome of *T. gamsii* T035 consisted of 30 contigs, with a total assembly length of 38.8 Mbp (N50 = 3.1 Mbp and N90 = 1.3 Mbp), a GC content of 48.44% and a largest contig of 7.09 Mbp. Those contigs were then assembled as 18 scaffolds, with a N50 of 7.18 Mb and a N90 of 4.03 Mb (Fig. 3 and Table I), introducing 3.09 N's per 100 kbp. Assembly completeness, assessed with BUSCO, indicated 98.8% complete universal genes (complete and single-copy: 98.3%; complete and duplicated: 0.5%; fragmented: 0.4%; missing: 0.8%) against the fungi_odb10 database (Fig. 3) (Tegenfeldt et al., 2025). The main genome metrics for *T. gamsii* strain T035 are compared with those of other published *T. gamsii* genomes in Table I.

Genome structural annotation and annotation quality control

Structural annotation was performed using the deep-learning tool Helixer (Holst et al., 2023), predicting 13,036 protein-coding genes. Compared to the previously published reference genome of *T. gamsii* T6085, annotated with MAKER2 (Holt & Yandell, 2011), *T. gamsii* T035 annotation identified over 2,000 additional protein-coding genes (Table II).

Table II: Genome annotation metrics comparing *T. gamsii* (strain T035) from this study with the reference genome *T. gamsii* (strain T6085) from Baroncelli et al. (2016). Asterisks indicate values reported in Baroncelli et al. (2016); values without asterisks were generated in this study. Secondary metabolite clusters were predicted using FungiSMASH. Carbohydrate-active enzymes (CAZymes) were identified using dbCAN2; only high-confidence enzymes are listed, defined as matches detected by all tested tools: HMMER: dbCAN (E-value < 1e-15, coverage > 0.35), DIAMOND: CAZy (E-value < 1e-102), and HMMER: dbCAN-sub (E-value < 1e-15, coverage > 0.35).

		***Trichoderma gamsii* strain T6085** Actual reference genome (Baroncelli et al., 2016)	***Trichoderma gamsii* strain T035** Genome from this study
	Structural annotation	MAKER2	Helixer
	Predicted protein-coding genes	10,944*	13,036
	Signal peptide	1,356*	1,046
Secondary metabolite	Isocyanide	2	2
	NRPS	14	11
	PKS	11	11
	Terpene	10	12
	Isocyanide-nrp	3	3
	PKS/NRPS	4	4
	NRPS/PKS/terpène	1	1
Carbohydrate-	Glucoside hydrolase (GH)	250	257
	Glycosyltransferase (GT)	87	88
	Polysaccharide Lyase (PL)	10	10
	Carbohydrate Esterase (CE)	19	20
	Carbohydrate-Binding Module (CBM)	33	33
	Auxiliary Activity (AA)	45	44

To evaluate annotation quality, we mapped RNA-seq reads from nine public transcriptomic datasets (Supplementary Table S3) to both the new and the previous annotations using STAR (Dobin et al. 2013). Mapping to the new annotation resulted in more than a 10% increase (from 64% to 75%) in reads assigned to annotated regions (present in the GTF file), demonstrating a substantial improvement in gene model accuracy (Table III). Interestingly, depending on the tested dataset, this increase ranged from 9% up to nearly 20% more reads mapping to annotated regions in T035 compared to T6085.

Table III: Evaluation of structural annotation for *T. gamsii* strain T035 (this study) and the reference genome *T. gamsii* strain T6085 (Baroncelli et al., 2016) using transcriptomic data from 9 public studies. Reads were mapped to both genomes using STAR, and the obtained mapping statistics are reported in this table as percentages. No major differences were observed in unmapped, multimapped, or ambiguously mapped reads between the two annotations. However, approximately 10% more reads aligned to annotated features in this study genome (regions present in the GTF annotation), which corresponded to a 10% decrease in reads mapping to unannotated regions ("No Feature").

		***Trichoderma gamsii* strain T6085** Actual reference genome (Baroncelli et al., 2016)	***Trichoderma gamsii* strain T035** Genome from this study
	Structural annotation	MAKER2	Helixer
Read mapping using STAR expressed in percentage	Unmapped	16.87	15.57
	Multimapped	0.88	1.62
	No Feature	17.73	5.38
	Ambiguous	0.22	2.42
	Mapped on Feature	64.30	75.02

249 Transposable element analysis revealed that only 3.3% of the T035 genome is composed of
250 transposable elements (Table IV and Supplementary Table S4). This proportion is low compared
251 to published TE contents in some other filamentous fungi, which can exceed 20% (e.g., *Blumeria*
252 *graminis*, *Leptosphaeria maculans*, *Fusarium graminearum*) (Ma et al., 2010; Spanu et al., 2010;
253 Grandaubert et al., 2014). The most abundant superfamilies were LTR retrotransposons of the
254 Gypsy type (0.51%), helitrons (0.58%), and TIR elements of the CACTA and Mutator families
255 (0.16% each). Other TE classes, including LINEs and SINEs, were only marginally represented
256 (<0.1%).

257 Table IV: Composition of transposable elements in *Trichoderma gamsii* strain T035
258 as determined with EDTA.

Class		Number of elements	Lenght occupied	% of sequence
LINE	Tad1	51	22715	0.06%
LTR	Gypsy	181	198697	0.51%
	unknown	78	99301	0.26%
SINE	tRNA	17	1754	0.00%
	unknown	15	1694	0.00%
TIR	CACTA	32	63747	0.16%
	Mutator	34	63446	0.16%
	PIF_Harbinger	8	13027	0.03%
	Tc1_Mariner	4	10557	0.03%
	hAT	1	1463	0.00%
nonTIR	helitron	24	224071	0.58%
rDNA	45S	13	6676	0.02%
repeat_fragment	–	797	573520	1.48%

259

260 **Genome functional annotation**

261 Functional annotation using EggNOG-mapper (Cantalapiedra et al., 2021) assigned functional
262 categories to 11,073 out of 13,036 predicted genes.
263 Secretome prediction identified 1,046 proteins with signal peptides using DeepSig (Savojardo
264 et al., 2018) (Table II). For comparison, 1,356 signal peptide-containing proteins were identified
265 with SignalP (Petersen et al., 2011) and previously reported in strain T6085 (Baroncelli et al.,
266 2016).
267 Secondary metabolite biosynthetic gene clusters were predicted in both *T. gamsii* strains T035
268 and T6085, with 44 and 45 clusters identified, respectively (Table II). The clusters comprised a
269 globally similar distribution of types, including NRPS, PKS, terpene, isocyanide, and mixed
270 NRPS/PKS clusters, reflecting comparable secondary metabolic potential in both strains.
271 Finally, carbohydrate-active enzymes (CAZymes) were identified with high confidence
272 (validated by HMMER, DIAMOND, and dbCAN_sub), resulting in the identification of 412 and 403
273 CAZymes in T035 and T6085, respectively (Table II).
274
275

Discussion

In this study, we generated the most contiguous genome assembly of the biocontrol fungus *T. gamsii* to date, with scaffold N50 and L50 values of 7.18 Mb and 3, respectively, compared to the previously best available assembly, which had an N50 of 697.4 kb and an L50 of 18 (Table I, Fig. 3). The high quality of the assembly and annotation was further supported by BUSCO analysis (Fig. 3) and by the consistency between predicted gene models and experimental transcriptomic data (Table III).

Trichoderma gamsii T035 exhibits strong biocontrol potential, outperforming a commercial *Trichoderma* strain in direct antagonism assays. We demonstrated that T035 secretes highly effective antibiotic compounds into its culture medium (Fig. 4B). Consistently, the genome harbors a rich repertoire of secondary metabolite clusters and carbohydrate-active enzymes, providing a molecular basis for these activities and offering prospects for future functional characterization.

Interestingly, strain T035 displayed strong activity, particularly against the Basidiomycete *R. solani* and the Ascomycete *Phoma* spp. However, this strain showed little to no activity against wood-decay fungi. In the case of *Globisporangium*, the situation appears more complex, as the activity levels are isolate-dependent (Fig. 4A). Such specificity recalls mechanisms described in plant-pathogenic fungi producing host-selective toxins, which are typically low-molecular-weight secondary metabolites (Hatta et al., 2002; Courtial et al., 2022), and/or deploying effectors, small cysteine-rich secreted proteins, that suppress host immunity (Ayukawa et al., 2021).While such mechanisms are well documented in phytopathogens, their occurrence in mycoparasitic interactions remains unclear. Nevertheless, we cannot exclude that similar principles might underlie the observed specificity of T035. In line with this idea, studies on *Trichoderma* suggest that its antagonistic activity can involve pathogen-dependent regulatory pathways (Sharma et al., 2017). We therefore speculate that the observed specificity of T035 against *Globisporangium* spp. could involve specialized attack pathways, possibly mediated by host-specific toxins and/or effectors (Ramírez-Valdespino et al., 2019), or alternatively reflect differences in host defense mechanisms. Confirming this hypothesis will require further investigations of the identified repertoire of secondary metabolite clusters, as well as the predicted set of secreted proteins.

Overall, this study provides a high-quality genome assembly of *T. gamsii* T035, including detailed annotation of protein-coding genes, secondary metabolite clusters, and carbohydrate-active enzymes. The *T. gamsii* T035 genome was estimated to have 13,036 protein-coding genes, while the actual public reference genome of *T. gamsii* (for the T6085 strain) contained 10,944 predicted genes. The draft genome sequence has been deposited in NCBI and is available in the BioProject PRJNA1327094. This genomic resource, together with the biological assays, will support future research aimed at elucidating the molecular basis of *T. gamsii* biocontrol activity and its potential applications in sustainable agriculture.

Acknowledgements

We thank the ANAN platform and the entire Nanopore Team, especially Muriel Bahut, Jessica Dimtter, Maryline Cournol, and Sandrine Balzergue, for the material and technical support during the genome sequencing.

Funding

The authors declare that they have received no specific funding for this study.

Conflict of interest disclosure

The authors declare that they comply with the PCI rule of having no financial conflicts of interest in relation to the content of the article.

Data, scripts, code, and supplementary information availability

Data, supplementary figure and tables, scripts, and code are available online on GitHub and stored with Zenodo: https://doi.org/10.5281/zenodo.17175563 (JustiCol, 2025)

T035 genomic data are available in NCBI BioProject PRJNA1327094.

References

Alonge M, Lebeigle L, Kirsche M, Jenike K, Ou S, Aganezov S, Wang X, Lippman ZB, Schatz MC, Soyk S (2022) Automated assembly scaffolding using RagTag elevates a new tomato system for high-throughput genome editing. *Genome Biology*, **23**, 258. https://doi.org/10.1186/s13059-022-02823-7

Anees M, Tronsmo A, Edel-Hermann V, Hjeljord LG, Héraud C, Steinberg C (2010) Characterization of field isolates of Trichoderma antagonistic against Rhizoctonia solani. *Fungal Biology*, **114**, 691–701. https://doi.org/10.1016/j.funbio.2010.05.007

Ayukawa Y, Asai S, Gan P, Tsushima A, Ichihashi Y, Shibata A, Komatsu K, Houterman PM, Rep M, Shirasu K, Arie T (2021) A pair of effectors encoded on a conditionally dispensable chromosome of Fusarium oxysporum suppress host-specific immunity. *Communications Biology*, **4**, 707. https://doi.org/10.1038/s42003-021-02245-4

Baroncelli R, Zapparata A, Piaggeschi G, Sarrocco S, Vannacci G (2016) Draft Whole-Genome Sequence of *Trichoderma gamsii* T6085, a Promising Biocontrol Agent of *Fusarium* Head Blight on Wheat. *Genome Announcements*, **4**, e01747-15. https://doi.org/10.1128/genomeA.01747-15

Bedine Boat MA, Sameza ML, Iacomi B, Tchameni SN, Boyom FF (2020) Screening, identification and evaluation of *Trichoderma* spp. for biocontrol potential of common bean damping-off pathogens. *Biocontrol Science and Technology*, **30**, 228–242. https://doi.org/10.1080/09583157.2019.1700909

Blin K, Shaw S, Vader L, Szenei J, Reitz ZL, Augustijn HE, Cediel-Becerra JDD, de Crécy-Lagard V, Koetsier RA, Williams SE, Cruz-Morales P, Wongwas S, Segurado Luchsinger AE, Biermann F, Korenskaia A, Zdouc MM, Meijer D, Terlouw BR, van der Hooft JJJ, Ziemert N, Helfrich EJN, Masschelein J, Corre C, Chevrette MG, van Wezel GP, Medema MH, Weber T (2025) antiSMASH 8.0: extended gene cluster detection capabilities and analyses of chemistry, enzymology, and regulation. *Nucleic Acids Research*, **53**, W32–W38. https://doi.org/10.1093/nar/gkaf334

Bunbury-Blanchette AL, Walker AK (2019) Trichoderma species show biocontrol potential in dual culture and greenhouse bioassays against Fusarium basal rot of onion. *Biological Control*, **130**, 127–135. https://doi.org/10.1016/j.biocontrol.2018.11.007

Cantalapiedra CP, Hernández-Plaza A, Letunic I, Bork P, Huerta-Cepas J (2021) eggNOG-mapper v2: Functional Annotation, Orthology Assignments, and Domain Prediction at the Metagenomic Scale (K Tamura, Ed,). *Molecular Biology and Evolution*, **38**, 5825–5829. https://doi.org/10.1093/molbev/msab293

Chateau C, Bastide F, Guillemette T, Hamon B, Longuemare M, Alexandre S, Buronfosse M, Roman H, Leduc N, Poupard P (2024) *In vitro* and *in vivo* biocontrol studies against *Botrytis cinerea* , the causal agent of grey mould in *Hydrangea macrophylla*. *Biocontrol Science and Technology*, **34**, 269–295. https://doi.org/10.1080/09583157.2024.2341302

Chen J-L, Sun S-Z, Miao C-P, Wu K, Chen Y-W, Xu L-H, Guan H-L, Zhao L-X (2016) Endophytic Trichoderma gamsii YIM PH30019: a promising biocontrol agent with hyperosmolar, mycoparasitism, and antagonistic activities of induced volatile organic compounds on root-rot pathogenic fungi of Panax notoginseng. *Journal of Ginseng Research*, **40**, 315–324. https://doi.org/10.1016/j.jgr.2015.09.006

Courtial J, Helesbeux J-J, Oudart H, Aligon S, Bahut M, Hamon B, N'Guyen G, Pigné S, Hussain AG, Pascouau C, Bataillé-Simoneau N, Collemare J, Berruyer R, Poupard P (2022) Characterization of NRPS and PKS genes involved in the biosynthesis of SMs in Alternaria dauci including the phytotoxic polyketide aldaulactone. *Scientific Reports*, **12**, 8155. https://doi.org/10.1038/s41598-022-11896-0

De Coster W, D'Hert S, Schultz DT, Cruts M, Van Broeckhoven C (2018) NanoPack: visualizing and processing long-read sequencing data (B Berger, Ed,). *Bioinformatics*, **34**, 2666–2669. https://doi.org/10.1093/bioinformatics/bty149

Dennis C, Webster J (1971) Antagonistic properties of species-groups of Trichoderma. *Transactions of the British Mycological Society*, **57**, 25-IN3. https://doi.org/10.1016/S0007-1536(71)80077-3

Dobin A, Davis CA, Schlesinger F, Drenkow J, Zaleski C, Jha S, Batut P, Chaisson M, Gingeras TR (2013) STAR: ultrafast universal RNA-seq aligner. *Bioinformatics*, **29**, 15–21. https://doi.org/10.1093/bioinformatics/bts635

Galletti S, Paris R, Cianchetta S (2020) Selected isolates of Trichoderma gamsii induce different pathways of systemic resistance in maize upon Fusarium verticillioides challenge. *Microbiological Research*, **233**, 126406. https://doi.org/10.1016/j.micres.2019.126406

Grandaubert J, Lowe RG, Soyer JL, Schoch CL, Van De Wouw AP, Fudal I, Robbertse B, Lapalu N, Links MG, Ollivier B, Linglin J, Barbe V, Mangenot S, Cruaud C, Borhan H, Howlett BJ, Balesdent M-H, Rouxel T (2014) Transposable element-assisted evolution and adaptation to host plant within the Leptosphaeria maculans-Leptosphaeria biglobosa species complex of fungal pathogens. *BMC Genomics*, **15**, 891. https://doi.org/10.1186/1471-2164-15-891

Hatta R, Ito K, Hosaki Y, Tanaka T, Tanaka A, Yamamoto M, Akimitsu K, Tsuge T (2002) A Conditionally Dispensable Chromosome Controls Host-Specific Pathogenicity in the Fungal Plant Pathogen *Alternaria alternata*. *Genetics*, **161**, 59–70. https://doi.org/10.1093/genetics/161.1.59

Holst F, Bolger A, Günther C, Maß J, Triesch S, Kindel F, Kiel N, Saadat N, Ebenhöh O, Usadel B, Schwacke R, Bolger M, Weber APM, Denton AK (2023) Helixer– *de novo* Prediction of Primary Eukaryotic Gene Models Combining Deep Learning and a Hidden Markov Model. https://doi.org/10.1101/2023.02.06.527280

Holt C, Yandell M (2011) MAKER2: an annotation pipeline and genome-database management tool for second-generation genome projects. *BMC Bioinformatics*, **12**, 491. https://doi.org/10.1186/1471-2105-12-491

Joubert A, Calmes* B, Berruyer R, Pihet M, Bouchara J-P, Simoneau P, Guillemette T (2010) Laser nephelometry applied in an automated microplate system to study filamentous fungus growth. *BioTechniques*, **48**, 399–404. https://doi.org/10.2144/000113399

JustiCol (2025) JustiCol/Genome-assembly-T_gamsii_T035: First submission. https://doi.org/10.5281/ZENODO.17175563

Katz L, Griswold T, Morrison S, Caravas J, Zhang S, Bakker H, Deng X, Carleton H (2019) Mashtree: a rapid comparison of whole genome sequence files. *Journal of Open Source Software*, **4**, 1762. https://doi.org/10.21105/joss.01762

Kolmogorov M, Yuan J, Lin Y, Pevzner PA (2019) Assembly of long, error-prone reads using repeat graphs. *Nature Biotechnology*, **37**, 540–546. https://doi.org/10.1038/s41587-019-0072-8

Koren S, Walenz BP, Berlin K, Miller JR, Bergman NH, Phillippy AM (2017) Canu: scalable and accurate long-read assembly via adaptive *k* -mer weighting and repeat separation. *Genome Research*, **27**, 722–736. https://doi.org/10.1101/gr.215087.116

Kumar S, Stecher G, Suleski M, Sanderford M, Sharma S, Tamura K (2024) MEGA12: Molecular Evolutionary Genetic Analysis Version 12 for Adaptive and Green Computing (FU Battistuzzi, Ed,). *Molecular Biology and Evolution*, **41**, msae263. https://doi.org/10.1093/molbev/msae263

Lee J, Huh N, Hong JH, Kim BS, Kim G-H, Kim J-J (2012) The antagonistic properties of Trichoderma spp. inhabiting woods for potential biological control of wood-damaging fungi. *Holzforschung*, **66**, 883–887. https://doi.org/10.1515/hf.2011.187

Lu H, Giordano F, Ning Z (2016) Oxford Nanopore MinION Sequencing and Genome Assembly. *Genomics, Proteomics & Bioinformatics*, **14**, 265–279. https://doi.org/10.1016/j.gpb.2016.05.004

Ma L-J, Van Der Does HC, Borkovich KA, Coleman JJ, Daboussi M-J, Di Pietro A, Dufresne M, Freitag M, Grabherr M, Henrissat B, Houterman PM, Kang S, Shim W-B, Woloshuk C, Xie X, Xu J-R, Antoniw J, Baker SE, Bluhm BH, Breakspear A, Brown DW, Butchko RAE, Chapman S, Coulson R, Coutinho PM, Danchin EGJ, Diener A, Gale LR, Gardiner DM, Goff S, Hammond-Kosack KE, Hilburn K, Hua-Van A, Jonkers W, Kazan K, Kodira CD, Koehrsen M, Kumar L, Lee Y-H, Li L, Manners JM, Miranda-Saavedra D, Mukherjee M, Park G, Park J, Park S-Y, Proctor RH, Regev A, Ruiz-Roldan MC, Sain D, Sakthikumar S, Sykes S, Schwartz DC, Turgeon BG, Wapinski I, Yoder O, Young S, Zeng Q, Zhou S, Galagan J, Cuomo CA, Kistler HC, Rep M (2010) Comparative genomics reveals mobile pathogenicity chromosomes in Fusarium. *Nature*, **464**, 367–373. https://doi.org/10.1038/nature08850

Marik T, Gufu B, Vishwanathula A, Balázs D, Rozsnyói Á, Terna G, Kovács F, Kocsubé S, Varga M, Szekeres A, Druzhinina IS, Vágvölgyi C, Papp T, Tyagi C, Kredics L (2025) Novel peptaibiotics identified from Trichoderma clade Viride. *Natural Products and Bioprospecting*, **15**, 48. https://doi.org/10.1007/s13659-025-00524-9

Migheli Q, Balmas V, Komoñ-Zelazowska M, Scherm B, Fiori S, Kopchinskiy AG, Kubicek CP, Druzhinina IS (2009) Soils of a Mediterranean hot spot of biodiversity and endemism (Sardinia, Tyrrhenian Islands) are inhabited by pan-European, invasive species of *Hypocrea/Trichoderma*. *Environmental Microbiology*, **11**, 35–46. https://doi.org/10.1111/j.1462-2920.2008.01736.x

Mikheenko A, Saveliev V, Hirsch P, Gurevich A (2023) WebQUAST: online evaluation of genome assemblies. *Nucleic Acids Research*, **51**, W601–W606. https://doi.org/10.1093/nar/gkad406

Möller EM, Bahnweg G, Sandermann H, Geiger HH (1992) A simple and efficient protocol for isolation of high molecular weight DNA from filamentous fungi, fruit bodies, and infected plant tissues. *Nucleic Acids Research*, **20**, 6115–6116. https://doi.org/10.1093/nar/20.22.6115

Pascouau C, Chateau C, Bastide F, Le Moullec-Rieu T, Guillemette T, Hamon B, Aligon S, Cailleau A, Sochard D, Gombert J, Morel E, Laurent E, Sérandat I, Berruyer R, Poupard P (2023) Characterization and pathogenicity of *Fusarium* spp. isolates causing root and collar rot on carrot. *Canadian Journal of Plant Pathology*, **45**, 76–91. https://doi.org/10.1080/07060661.2022.2103737

Petersen TN, Brunak S, Von Heijne G, Nielsen H (2011) SignalP 4.0: discriminating signal peptides from transmembrane regions. *Nature Methods*, **8**, 785–786. https://doi.org/10.1038/nmeth.1701

Ramírez-Valdespino CA, Casas-Flores S, Olmedo-Monfil V (2019) Trichoderma as a Model to Study Effector-Like Molecules. *Frontiers in Microbiology*, **10**, 1030. https://doi.org/10.3389/fmicb.2019.01030

Rinu K, Sati P, Pandey A (2014) *Trichoderma gamsii* (NFCCI 2177): A newly isolated endophytic, psychrotolerant, plant growth promoting, and antagonistic fungal strain. *Journal of Basic Microbiology*, **54**, 408–417. https://doi.org/10.1002/jobm.201200579

Savojardo C, Martelli PL, Fariselli P, Casadio R (2018) DeepSig: deep learning improves signal peptide detection in proteins (A Valencia, Ed,). *Bioinformatics*, **34**, 1690–1696. https://doi.org/10.1093/bioinformatics/btx818

Sharma V, Salwan R, Sharma PremN, Kanwar SS (2017) Elucidation of biocontrol mechanisms of Trichoderma harzianum against different plant fungal pathogens: Universal yet host specific response. *International Journal of Biological Macromolecules*, **95**, 72–79. https://doi.org/10.1016/j.ijbiomac.2016.11.042

Spanu PD, Abbott JC, Amselem J, Burgis TA, Soanes DM, Stüber K, Loren Van Themaat EV, Brown JKM, Butcher SA, Gurr SJ, Lebrun M-H, Ridout CJ, Schulze-Lefert P, Talbot NJ, Ahmadinejad N, Ametz C, Barton GR, Benjdia M, Bidzinski P, Bindschedler LV, Both M, Brewer MT, Cadle-Davidson L, Cadle-Davidson MM, Collemare J, Cramer R, Frenkel O, Godfrey D, Harriman J, Hoede C, King BC, Klages S, Kleemann J, Knoll D, Koti PS, Kreplak J, López-Ruiz

FJ, Lu X, Maekawa T, Mahanil S, Micali C, Milgroom MG, Montana G, Noir S, O'Connell RJ, Oberhaensli S, Parlange F, Pedersen C, Quesneville H, Reinhardt R, Rott M, Sacristán S, Schmidt SM, Schön M, Skamnioti P, Sommer H, Stephens A, Takahara H, Thordal-Christensen H, Vigouroux M, Weßling R, Wicker T, Panstruga R (2010) Genome Expansion and Gene Loss in Powdery Mildew Fungi Reveal Tradeoffs in Extreme Parasitism. *Science*, **330**, 1543–1546. https://doi.org/10.1126/science.1194573

Su W, Ou S, Hufford MB, Peterson T (2021) A Tutorial of EDTA: Extensive De Novo TE Annotator. In: *Plant Transposable Elements* Methods in Molecular Biology. (ed Cho J), pp. 55–67. Springer US, New York, NY. https://doi.org/10.1007/978-1-0716-1134-0_4

Tegenfeldt F, Kuznetsov D, Manni M, Berkeley M, Zdobnov EM, Kriventseva EV (2025) OrthoDB and BUSCO update: annotation of orthologs with wider sampling of genomes. *Nucleic Acids Research*, **53**, D516–D522. https://doi.org/10.1093/nar/gkae987

Valan Arasu M, Vijayaraghavan P, Al-Dhabi NA, Choi KC, Moovendhan M (2023) Biocontrol of *Trichoderma gamsii* induces soil suppressive and growth-promoting impacts and rot disease-protecting activities. *Journal of Basic Microbiology*, **63**, 801–813. https://doi.org/10.1002/jobm.202300016

Vaser R, Sović I, Nagarajan N, Šikić M (2017) Fast and accurate de novo genome assembly from long uncorrected reads. https://doi.org/10.1101/gr.214270.116

Warringer J, Blomberg A (2003) Automated screening in environmental arrays allows analysis of quantitative phenotypic profiles in *Saccharomyces cerevisiae*. *Yeast*, **20**, 53–67. https://doi.org/10.1002/yea.931

Zheng J, Ge Q, Yan Y, Zhang X, Huang L, Yin Y (2023) dbCAN3: automated carbohydrate-active enzyme and substrate annotation. *Nucleic Acids Research*, **51**, W115–W121. https://doi.org/10.1093/nar/gkad328